

# Mueller Matrix Polarimetry: A Powerful Tool for Nanostructure Metrology

Shiyuan Liu<sup>\*</sup>, Xiuguo Chen, and Chuanwei Zhang

State Key Laboratory of Digital Manufacturing Equipment and Technology,  
Huazhong University of Science and Technology, Wuhan 430074, China

<sup>\*</sup>Corresponding author: [shyliu@mail.hust.edu.cn](mailto:shyliu@mail.hust.edu.cn)

Recently, ellipsometry-based scatterometry has gained more and more attention in semiconductor manufacturing. Among the various types of ellipsometry, Mueller matrix polarimetry (MMP) can obtain up to 16 quantities of a 4×4 Mueller matrix, and consequently, MMP-based scatterometry can acquire much more useful information about the sample. In this paper, the basic principle and instrumentation of MMP are presented, and then the fundamental concept of computational metrology is introduced. Several case studies are finally provided to demonstrate the potential of MMP in nanostructure metrology.

## 1. Introduction

Recently, ellipsometry-based scatterometry has been introduced to monitor the critical dimension (CD) and overlay of grating structures in semiconductor manufacturing [1-3]. It measures the change of ellipsometric angles in the zeroth-order diffracting beam that is scattered from the periodic structure. Among the various types of ellipsometry, Mueller matrix polarimetry (MMP), can obtain up to 16 quantities of a 4×4 Mueller matrix. Consequently, MMP-based scatterometry can acquire much more useful information about the sample and thereby can achieve better measurement sensitivity and accuracy than the conventional ellipsometric scatterometry [4-6]. MMP is thus expected to provide a powerful tool for nanostructure metrology in high-volume manufacturing.

In this paper, we present the principle and potential of MMP in nanostructure metrology. We first introduce the basic principle and instrumentation of MMP, with a demonstration of the development of a dual rotating-compensator MMP in our lab. Then we put forward the concept of computational metrology, and point out that MMP-based nanometrology is essentially a model-based technique by modeling a complicated forward process followed by solving a corresponding inverse problem. Finally, we provide several case studies in MMP-based nanostructure metrology, including photoresist nanostructures with line edge roughness (LER) and nanoimprinted grating structures. These studies reveal the capability of MMP in nanostructure metrology.

## 2. Instrumentation of Mueller Matrix Polarimetry

A dual rotating-compensator configuration is adopted to measure the sample Mueller matrices. As schematically shown in Fig. 1, the system layout of the dual rotating-

compensator MMP in order of light propagation is  $PC_{r1}(\omega_1)SC_{r2}(\omega_2)A$ , where P and A stand for the polarizer and analyzer,  $C_{r1}$  and  $C_{r2}$  refer to the 1st and 2nd rotating compensators, and S stands for the sample. The 1st and 2nd compensators rotate synchronously at  $\omega_1 = 5\omega$  and  $\omega_2 = 3\omega$ , where  $\omega$  is the fundamental mechanical frequency. The emerging Stokes vector  $\mathbf{S}_{out}$  of the light beam can be expressed as the following Mueller matrix product [7-9]

$$\mathbf{S}_{out} = [\mathbf{M}_A \mathbf{R}(A)] [\mathbf{R}(-C_2) \mathbf{M}_{C_2}(\delta_2) \mathbf{R}(C_2)] \mathbf{M}_S [\mathbf{R}(-C_1) \mathbf{M}_{C_1}(\delta_1) \mathbf{R}(C_1)] [\mathbf{R}(-P) \mathbf{M}_P] \mathbf{S}_{in}, \quad (1)$$

where  $\mathbf{R}(\alpha)$  and  $\mathbf{M}_\beta$  are the corresponding rotation and Mueller matrices for each optical element. The angle  $\alpha$  in  $\mathbf{R}(\alpha)$  describes the orientation angles of the associated optical elements.  $\delta_1$  and  $\delta_2$  are the phase retardances of the 1st and 2nd rotating compensators. By performing Hadamard analysis [10], we can finally extract the sample Mueller matrix elements from the harmonic coefficients of the irradiance at the detector (proportional to the first element of the emerging Stokes vector  $\mathbf{S}_{out}$ ). Based on the above measurement principle, we have developed a MMP prototype suitable from ultraviolet to infrared spectral bands, as depicted in Fig. 1. Data analysis is performed using in-house developed optical modeling software based on rigorous coupled-wave analysis (RCWA) [11-13].

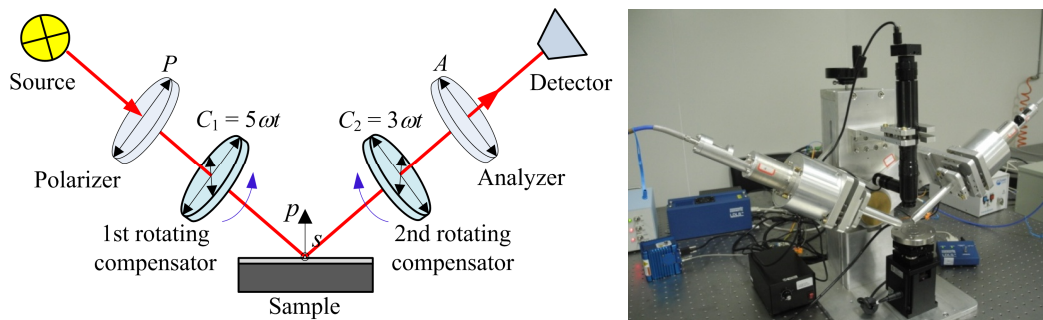


Figure 1. Principle and prototype of the dual rotating-compensator MMP

### 3. Concept of Computational Metrology

In the MMP-based nanostructure metrology, the optical signature of the nanostructure is measured first and then an optical model corresponding to the nanostructure is constructed. The next step, parameter extraction, involves an inverse diffraction problem solving. In this step, the calculated signature based on the constructed optical model is adjusted iteratively to find a signature that can best match the measured one. The structural parameters corresponding to the best matched signature will be treated as the final measurement results.

The MMP-based nanostructure metrology is essentially model-based metrology and heavily relies on two key techniques, i.e., the forward optical modeling and the inverse parameter extraction, which are both computationally intensive. Recently, we termed such kind of model-based metrology as *computational metrology* [14, 15], with an emphasis on solving the vast and complicated scientific computations, especially numerical computations. We summarize the fundamental principles of computational metrology, whose basic elements include the measurands, measurement configuration, forward model, measured data, and solution of measurands, as shown in Fig. 2. We also emphasize that the computational metrology should include at least three fundamental characteristics as follows:

(1) Computational metrology is essentially a model-based metrology, whose measurement system requires a complicated forward transfer model with multiple input and output parameters.

(2) Computational metrology is typically an inverse problem solving process, and its success heavily relies on two key techniques. One is the forward modeling and its fast algorithm, and the other is the inverse problem solving and its robust algorithm.

(3) The objective of computational metrology is quantitative measurement. The final solution of the measurands should and could be quantitatively evaluated by measurement error, accuracy, precision, and/or uncertainty.

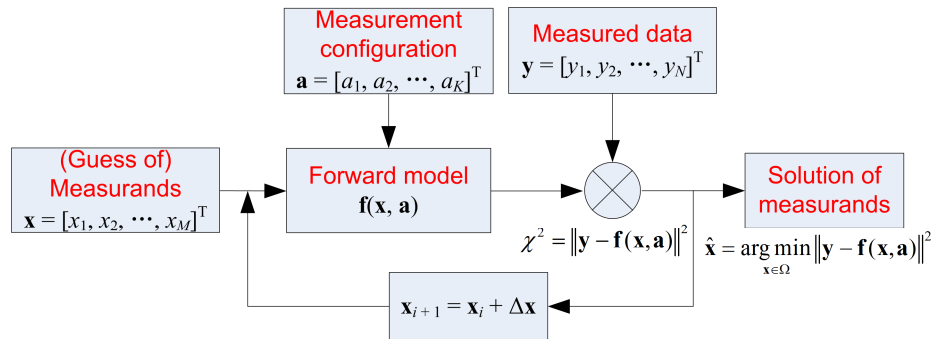


Figure 2. Fundamental concept and basic elements of computational metrology

#### 4. Mueller Matrix Polarimetry for Nanostructure Metrology

We have applied MMP to measure several types of nanostructures, including the two typical structures demonstrated in this paper. One is a photoresist grating structure with line edge roughness (LER), and the other is a nanoimprinted grating structure.

##### 4.1. Measurement of photoresist gratings with LER

As shown in Fig. 3, the investigated photoresist grating is characterized by top critical dimension  $TCD$ , sidewall angle  $SWA$ , grating height  $Hgt_1$ , and period  $pitch$ . The thickness of the bottom anti-reflective coating (BARC) layer is represented by  $Hgt_2$ . In the data analysis, rough edges of grating lines were approximated as effective medium boundary layers with thickness  $\sigma$ . This approximation simplifies the rough grating to one-dimensional (1D) periodic structures. We can perform simulations using a 1D RCWA solution. Table 1 presents the comparison of fitting parameters extracted from MMP and SEM measurements. Figure 4 depicts the fitting result of the calculated and polarimeter-measured Mueller matrix spectra. The results shown in Table 1 and Fig. 4 demonstrate the capability of MMP for accurate quantification of photoresist gratings with LER.

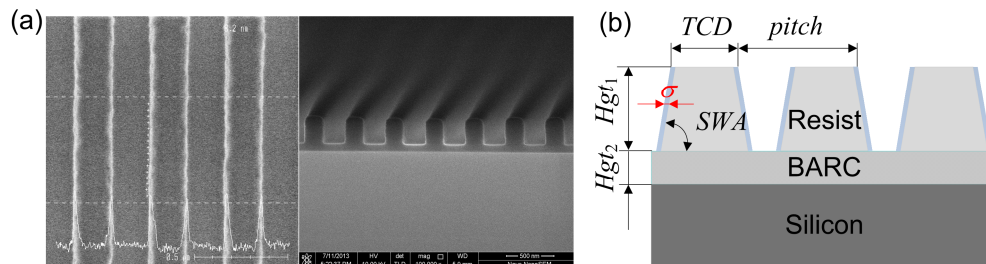


Figure 3. (a) CD-SEM and X-SEM micrographs and (b) geometric model of the investigated photoresist grating structure.

Table 1. Comparison of fitting parameters of the investigated photoresist grating structure extracted from the MMP and SEM measurements.

Parameters	MMP	SEM
$TCD$ (nm)	$201.39 \pm 2.485$	201.4
$Hgt_1$ (nm)	$310.27 \pm 0.374$	308.3
$SWA$ (deg)	$89.98 \pm 0.121$	89.3
$Hgt_2$ (nm)	$116.80 \pm 0.186$	115.4
$\sigma$ (nm)	$5.45 \pm 1.006$	3.6

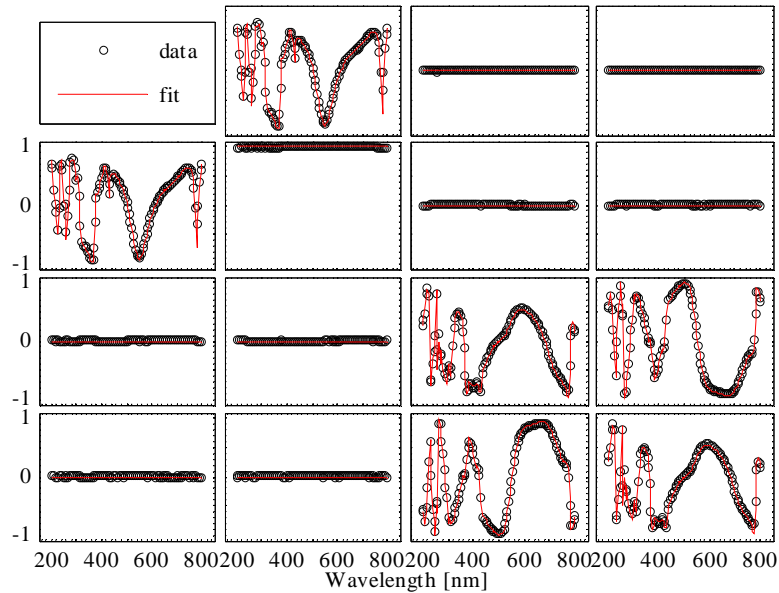


Figure 4. Fitting result of the calculated and polarimeter-measured Mueller matrix spectra for the investigated photoresist grating structure. The Mueller matrix elements are normalized to  $m_{11}$ , which is not shown. The incidence and azimuthal angles are fixed at  $65^\circ$  and  $0^\circ$ , respectively.

#### 4.2. Measurement of nanoimprinted grating structures

As shown in Fig. 5, the investigated nanoimprinted grating structure is characterized by a two-layer trapezoidal model with a total of six structural parameters  $p_1 \sim p_6$ , where the residual layer thickness is represented by  $p_6$ . Table 2 presents the comparison of fitting parameters of the nanoimprinted grating structure extracted from MMP and SEM measurements. Figure 6 depicts the fitting result of the calculated and polarimeter-measured Mueller matrix spectra when taking into account the depolarization effects induced by numerical aperture, finite spectral bandwidth, and residual layer thickness nonuniformity. The results shown in Table 2 and Fig. 6 demonstrate that MMP can not only be applied to accurately quantify the line width, line height, and residual layer thickness of the nanoimprinted gratings, but also to directly determine the variation in the residual layer thickness over the illumination spot [16].

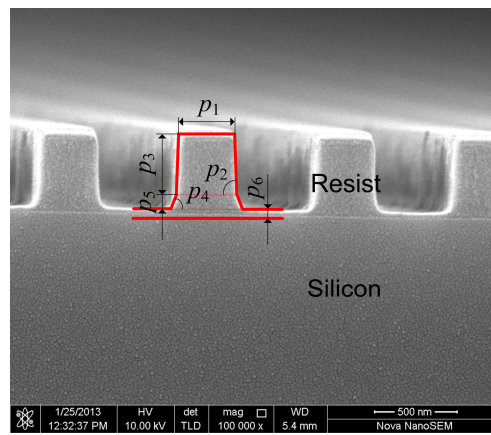


Figure 5. X-SEM micrograph and geometric model of the investigated nanoimprinted grating structure.

Table 2. Comparison of fitting parameters of the investigated nanoimprinted grating structure extracted from the MMP and SEM measurements.

Parameters	MMP	SEM
$p_1$ (nm)	$352.29 \pm 0.160$	352.2
$p_2$ (deg)	$87.11 \pm 0.026$	87.5
$p_3$ (nm)	$442.83 \pm 1.008$	
$p_4$ (deg)	$25.41 \pm 1.473$	472.1 <sup>a</sup>
$p_5$ (nm)	$29.65 \pm 0.973$	
$p_6$ (nm)	$61.41 \pm 0.077$	57.8
$\sigma_i$ (nm)	$3.19 \pm 0.060$	...

<sup>a</sup>This value corresponds to the total grating height, i.e.,  $p_3 + p_5$ .

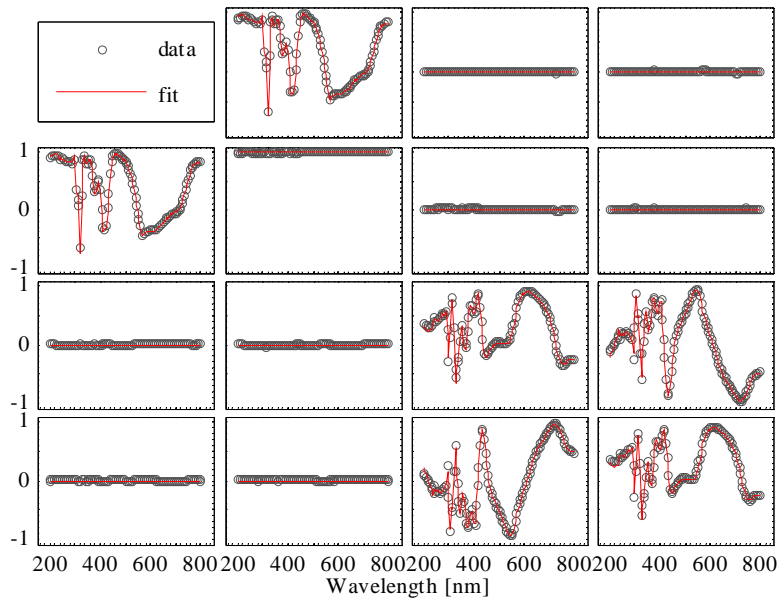


Figure 6. Fitting result of the calculated and polarimeter-measured Mueller matrix spectra for the investigated nanoimprinted grating structure when considering the depolarization effects induced by numerical aperture, finite spectral bandwidth, and residual layer thickness nonuniformity. The incidence and azimuthal angles are fixed at  $65^\circ$  and  $0^\circ$ , respectively.

## 5. Conclusions

In summary, we have presented the basic principle and instrumentation of MMP, with a demonstration of the development of a dual rotating-compensator MMP in our lab. By introducing the fundamental concept of computational metrology, we point out that the MMP-based nanometrology is essentially a model-based technique by modeling a complicated forward process followed by solving a corresponding inverse problem. We have applied MMP to measure several typical nanostructures, including the photoresist gratings with LER and nanoimprinted grating structures. These case studies have demonstrated the capability of MMP in nanostructure metrology. It is expected that MMP will provide a powerful tool for nanostructure metrology in future high-volume manufacturing.

## Acknowledgments

This work was funded by the National Natural Science Foundation of China (Grant Nos. 91023032, 51005091) and the National Instrument Development Specific Project of China (Grant No. 2011YQ160002).

## References

1. C. J. Raymond, M. R. Murnane, S. L. Prins, S. Sohail, H. Naqvi, J. R. McNeil, and J. W. Hosch, *J. Vac. Sci. Technol. B*, **15**(2), 361 (1997)
2. X. Niu, N. Jakatdar, J. Bao, and C. J. Spanos, *IEEE Trans. Semicond. Manuf.*, **14**(2), 97 (2001).
3. C. H. Ko and Y. S. Ku, *Opt. Express* **14**(13), 6001 (2006).
4. T. Novikova, A. De Martino, P. Bulkin, Q. Nguyen, B. Drévillon, V. Popov, and A. Chumakov, *Opt. Express*, **15**(5), 2033 (2007).
5. Y. N. Kim, J. S. Paek, S. Rabello, S. B. Lee, J. T. Hu, Z. Liu, T. D. Hao, and W. McGahan, *Opt. Express*, **17**(23), 21336 (2009).
6. X. G. Chen, S. Y. Liu, C. W. Zhang, and H. Jiang, *J. Micro/Nanolith. MEMS MOEMS*, **12**(3), 033013 (2013).
7. R. W. Collins and J. Koh, *J. Opt. Soc. Am. A*, **16**(8), 1997 (1999).
8. W. C. Du, S. Y. Liu, C. W. Zhang, and X. G. Chen, *Proc. SPIE*, **8759**, 875925 (2013).
9. W. Q. Li, S. Y. Liu, C. W. Zhang, and X. G. Chen, *Proc. SPIE*, **8759**, 875954 (2013).
10. H. Fujiwara, *Spectroscopic Ellipsometry: Principles and Applications*, Wiley (2007), chap. 4.
11. M. G. Moharam, E. B. Grann, D. A. Pommet, and T. K. Gaylord, *J. Opt. Soc. Am. A*, **12**(5), 1068 (1995).
12. L. Li, *J. Opt. Soc. Am. A*, **14**(10), 2758 (1997).
13. S. Y. Liu, Y. Ma, X. G. Chen, and C. W. Zhang, *Opt. Eng.*, **51**(8), 081504 (2012).
14. S. Y. Liu, *Proceedings of the 6th IEEE International Conference on Nano/Micro Engineered and Molecular Systems*, 1093 (2011).
15. S. Y. Liu, *Proc. SPIE*, **8916**, 891606 (2013).
16. X. G. Chen, C. W. Zhang, and S. Y. Liu, *Appl. Phys. Lett.* **103**(15), 151605 (2013).